Local surface elastic constants by resonant-ultrasound microscopy

Jiayong Tian,[a] Hirotsugu Ogi, Toyokazu Tada, and Masahiko Hirao
Graduate School of Engineering Science, Osaka University, Machikaneyama 1-3, Toyonaka, Osaka 560-8531, Japan

Hassel Ledbetter
Los Alamos National Laboratory (E536), Los Alamos, New Mexico 87545

(Received 18 February 2004; accepted 7 April 2004)

We report a method—*resonant-ultrasound microscopy*—for measuring elastic-constant distribution over a solid's surface. Applying an oscillating electric field to a rectangular-parallelepiped oscillator of langasite ($La_3Ga_5SiO_{14}$) crystal by a surrounding solenoid coil, we generated and detected vibrations of the crystal without electrodes and without wires. Acoustic coupling of the specimen to the oscillator is only made at an antinodal vibration point on the crystal's bottom surface. The crystal's resonance-frequency shift reflects elastic constants of the specimen in the contacting area. Point-contact measurement permits sensitive, quantitative evaluation of a material's local elastic constants. As an illustrating example, we measured the elastic-stiffness distribution of a Nb–Ti/Cu resin superconductive wire. We compared our measurements with both static-contact and dynamic-contact models. © *2004 American Institute of Physics.* [DOI: 10.1063/1.1755432]

I. INTRODUCTION

Recently, multiphase composites have been widely produced as functional and intelligent materials, which often contain microscale and nanoscale components. Mechanical properties of individual components are required because they govern the composite's macroscopic mechanical properties. Especially, elastic constants represent indispensable structural design parameters.

Many small-scale components show inhomogeneous microstructure and elastic anisotropy, thus a distribution of elastic constants. For example, silicon–carbide fiber shows a multilayer microstructure, and its elastic constants vary strongly along the radial direction.[1] Thus, measurement of elastic constants in a local area within a component assumes a central importance. One candidate measurement method is acoustic microscopy using a high-frequency surface wave.[2] However, surface roughness and a material's anisotropy make it difficult to measure wave velocities accurately. Also, it needs a couplant such as water. Recently, ultrasonic atomic force microscopy (UAFM) has been developed to measure the elastic property in microscale and nanoscale regions.[3,4] This method uses flexural vibration of a microscale cantilever. The tip attached at the free end taps the specimen surface with an applied force. The cantilever's resonance-frequency shift is related to the specimen's elastic properties.

However, the resonance frequency depends strongly on many factors, including the contacting piezoelectric transducer and gripping condition at the fixed end, preventing one from deducing the elastic constant of the specimen quantitatively.

Here, we present an alternative acoustic microscopy, *resonant-ultrasound microscopy* (RUM), to evaluate a material's local stiffness. This method uses the resonance-frequency shift of a rectangular-parallelepiped piezoelectric crystal (langasite, $La_3Ga_5SiO_{14}$) touching the specimen only at an anti-nodal point. The piezoelectric material's vibrations are excited and detected through dynamic electric fields using a surrounding solenoid coil. Thus, neither electrode nor mechanical contact is required for the acoustic coupling. Such noncontact excitation and detection of ultrasonic vibrations eliminates the measurement errors associated with contact coupling and ambiguous boundary conditions at the supports. Scanning the object surface with this probe and measuring the resonance frequency then provides an image of elastic-stiffness distribution. We consider the elastic-coefficient mapping of a Nb–Ti/Cu-resin-composite superconductive wire.

II. RESONANT-ULTRASOUND MICROSCOPY

Figure 1 shows the measurement setup of RUM. An oriented rectangular-parallelepiped langasite crystal was located within a solenoid coil, whose crystallographic X axis (a axis) is oriented vertically. The dimensions of the crystal along the X, Y, and Z axes are 4.954, 5.769, and 4.016 mm, respectively. Langasite possessed trigonal symmetry with point group 32, showing six elastic constants C_{ij}, two piezoelectric coefficients e_{ij}, and two dielectric coefficients ε_{ij} as given in Table I. Langasite's piezoelectric coefficients (two times larger than those of quartz) promise effective generation of vibration[5] by applying a contactless dynamic electric field. Furthermore, its elastic constants show weak temperature dependence (of the order of $10^{-5}\,K^{-1}$), assuring stable resonance frequencies.[6]

Because langasite's Young's modulus along the X and Y directions is smaller than that in the Z direction, we kept the X faces parallel to the specimen's surface fixed on a stage to obtain high sensitivity. (As shown below, a smaller oscilla-

[a]Author to whom correspondence should be addressed; electronic mail: j_tian@me.es.osaka-u.ac.jp

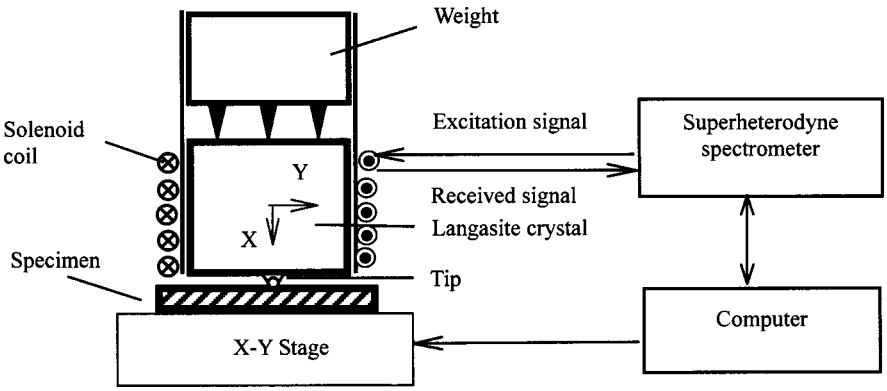

FIG. 1. Measurement setup of resonant-ultrasound microscopy (RUM).

tor's Young's modulus shows higher sensitivity to the specimen's Young's modulus.) The crystal touches the specimen through a tungsten–carbide spherical bearing with radius R bonded at the center of the bottom surface. A biasing force F_0 acts on the upper surface through needles to increase the sensitivity. (The sensitivity increases with increasing biasing force.) To eliminate their influence on vibration, the needles are located on the nodal line of vibration.

An oscillating electric field is generated by applying tone bursts to the solenoid coil, which excite vibrations of the crystal by the converse piezoelectric effect.[5] The vibrations are received by the same solenoid coil with the piezoelectric effect after the excitation. A superheterodyne spectrometer extracts the in-phase and out-of-phase components of the receiving signal to calculate the amplitude from the root of the sum of their squares.[7,8] Thus, a frequency scan provides a resonance spectrum (Fig. 2). Moving the stage by a stepping motor keeping the crystal/specimen contact produces a two-dimensional image of elastic-stiffness distribution.

III. MODAL ANALYSIS

We consider the sensitivity of the resonance frequency to the specimen's elastic constants. We assume Hertzian contact[3,4] for the tip-specimen contact and replace it with elastic springs shown in Fig. 3. The previous ultrasonic atomic force microscopy (UAFM) studies[3,4] used a simple static Hertz-contact model to calculate the effective contact stiffness as

$$k_{22}^s = k_{33}^s = 8G^* a, \tag{1a}$$

$$k_{11}^s = \sqrt[3]{6F_0 R E^{*2}}. \tag{1b}$$

Here $G^{*-1} = (2-\nu_1)G_1^{-1} + (2-\nu_2)G_2^{-1}$ and $E^{*-1} = (1-\nu_1^2)E_1^{-1} + (1-\nu_2^2)E_2^{-1}$. E, G, and ν represent Young's modulus, shear modulus, and Poisson's ratio, respectively. Subscripts 1 and 2 indicate the bearing and the specimen, respectively; $a = \sqrt[3]{3F_0 R/4E^*}$ denotes the contact radius. R is the bearing's radius. Recently, we showed experimentally and theoretically that this static model failed to explain the contact stiffness because of larger resistance of the interface deformation to the dynamic response associated with mass density and viscosity of the contacting materials.[9] Thus, the *dynamic* spring constants are usually larger than the static spring constants, although their analytical derivation is very complicated. We therefore approximate the spring stiffness as

$$k_{22} = k_{33} = \beta k_{22}^s, \tag{2a}$$

$$k_{11} = \alpha k_{11}^s. \tag{2b}$$

We consider the Lagrangian L in a piezoelectric material to calculate the resonance frequencies and vibration modes

$$L = \frac{1}{2}\int\int\int_{\Omega} (S_{ij}C_{ijkl}S_{kl} + 2S_{ij}e_{ijk}\phi_{,k} - \phi_{,i}\varepsilon_{ij}\phi_{,j} - \rho\omega^2 u_i u_i)dV + \frac{1}{2}\int\int_{\Gamma} K_{ij}u_j u_i dS, \tag{3}$$

Here S_{ij}, ρ, u_i, and ϕ_i denote the strain tensor, mass density, displacement, and electric potential, respectively. Ω and Γ denote the volume and the surface of the piezoelectric

TABLE I. Elastic constants C_{ij} (GPa), piezoelectric coefficients e_{ij} (C/m^2), and dielectric coefficients $\varepsilon_{ij}/\varepsilon_0$ of langasite (ε_0 denotes the dielectric constant of vacuum) (see Ref. 5).

C_{11}	C_{33}	C_{12}	C_{13}	C_{14}	C_{44}	e_{11}	e_{14}	$\varepsilon_{11}/\varepsilon_0$	$\varepsilon_{33}/\varepsilon_0$
189.5	262.6	105.3	97.16	14.25	53.5	−0.397	0.203	19.04	50.51

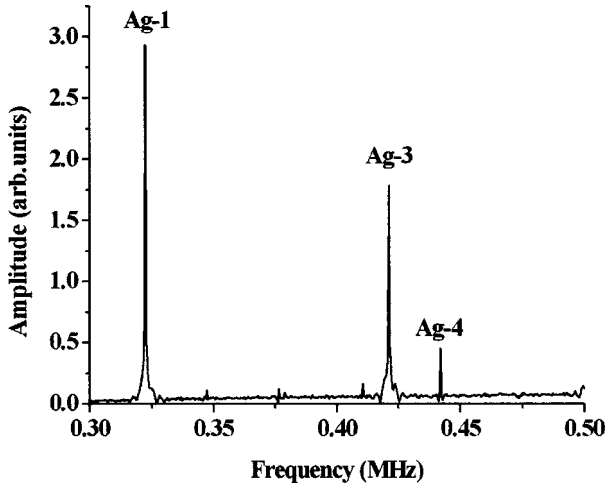

FIG. 2. Free-vibration resonance spectrum of a langasite probe measured with electric coupling to a solenoid coil.

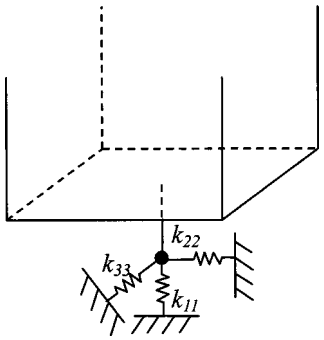

FIG. 3. Contact model of RUM.

crystal, respectively. K_{ij} denotes the spring constant per unit area, thus, $k_{11}=K_{11}\delta(x-x_0)dS$, for example; δ denotes Kronecker's delta and x_0 denotes the position of the point contact. Approximating the displacement and electric potential in terms of linear combinations of the basis functions consisting of normalized Legendre polynomials, the stationary point of the Lagrangian provides the resonance modes (Rayleigh–Ritz method).[5,8,10] Equation (3) shows that increasing the specimen's elastic stiffness increases the resonance frequency of the piezoelectric crystal.

Free vibrations of an oriented rectangular parallelepiped of langasite fall into four groups labeled A_g, A_u, B_g, and B_u.[10] We adopted the A_g-1 mode for the present study for two reasons: (1) We calculated the sensitivity of many modes in the four groups to the stiffnesses k_{11}, k_{22}, and k_{33} and found that mode A_g-1 shows the largest sensitivity to the normal contact stiffness k_{11} (Fig. 4) but negligible sensitivity to the tangential contact stiffness k_{22} and k_{33}. This is because the normal displacement u_1 of the A_g-1 mode shows an antinode at the center of the bottom surface, and in-plane displacements u_2 and u_3 show central nodal lines as shown in Fig. 5. The A_g-1 mode shows the vibration similar to a longitudinal vibration along the X axis. The biasing force F_0 is applied at three points on the calculated nodal lines of the top surface. (2) The A_g-1 mode is easily excited and shows a good spectrum shape as shown in Fig. 2.

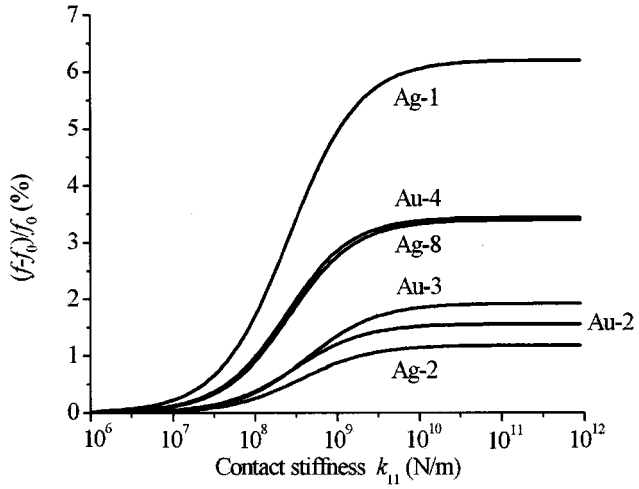

FIG. 4. Mode sensitivity to the contact stiffness k_{11}.

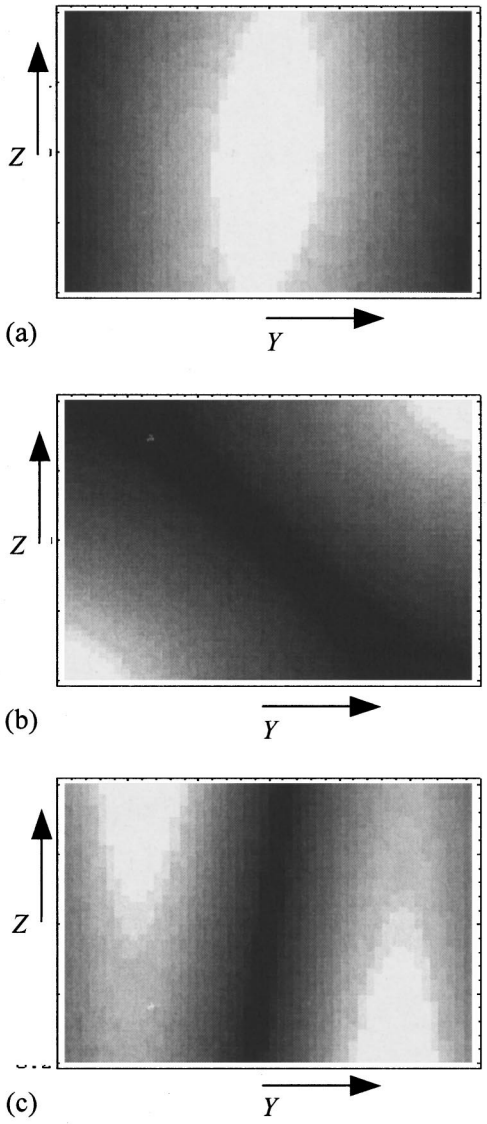

FIG. 5. Distribution of displacements of A_g-1 vibration mode at the upper surface of the probe calculated by the Rayleigh–Ritz method. (a) Displacement u_1, (b) displacement u_2, (c) displacement u_3.

IV. RESULTS AND DISCUSSION

To illustrate the usefulness of the proposed method, we scanned the cross section of a Nb–Ti/Cu–polyvinyl–resin superconductive wire[11,12] with a biasing force $F_0=0.13$ N. Figure 6 shows the cross section observed by optical microscopy. A single wire contains 180 NbTi filaments with a diameter of 32 μm in an oxygen-free copper matrix with 0.58 by 0.68 mm^2 cross section. The NbTi filament consists of 38.7 at.% Nb and 61.3 at.% Ti. Polyvinyl resin coats the wires.

Figure 7 shows an RUM image. The resonance frequency was measured at 5 μm steps. As reported elsewhere,[11] the averaged-a-direction Young's modulus for the copper matrix is 128.7 GPa and that for the NbTi filament is 84.3 GPa. A line trace of the frequency shift is shown in Fig. 8. We compare the measurements of the resonance frequency shift with those calculated by the dynamic-contact and static-contact models in Fig. 9 (here, $f_0=0.31894$ MHz

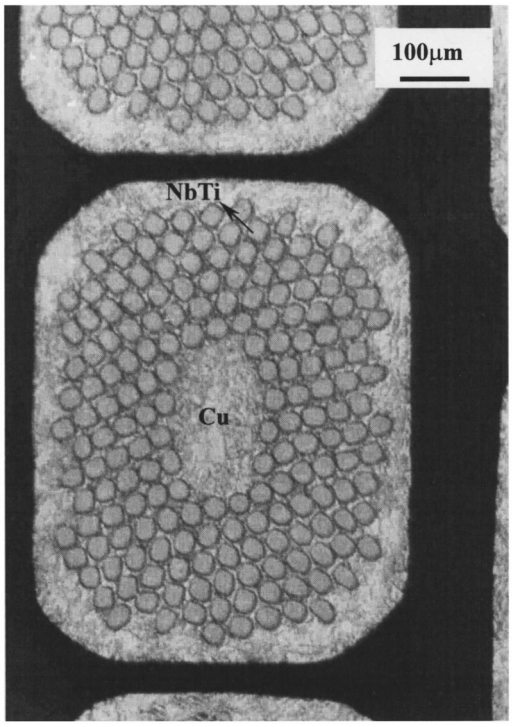

FIG. 6. Optical microstructure of a Nb–Ti/Cu/resin-composite superconductive wire.

is free-vibration resonance frequency of langasite). Here we used the averaged Young's modulus of copper and NbTi in our calculation. Scattering of the measurement of the copper matrix and NbTi filaments arises from different grain orientations. Because of its high anisotropy, copper Young's modulus can vary between 66.7 and 190.8 GPa depending on the grain orientation. Also, Young's modulus of NbTi (bcc phase at room temperature) varies between 63.6 and 107.6 GPa.[13] Our previous study with a different crystal and different vibration mode[14] revealed that $\alpha=3.6$ yields a best fit with the measurements. Furthermore, our theoretical study[9] with a sphere oscillator predicts $\alpha=2.4$. The dynamic model in Fig. 9 agrees well with the measurement within the error limits when $\alpha=3.3$. Thus, it appears that the dynamic-contact stiffness is larger than the static-contact stiffness by a

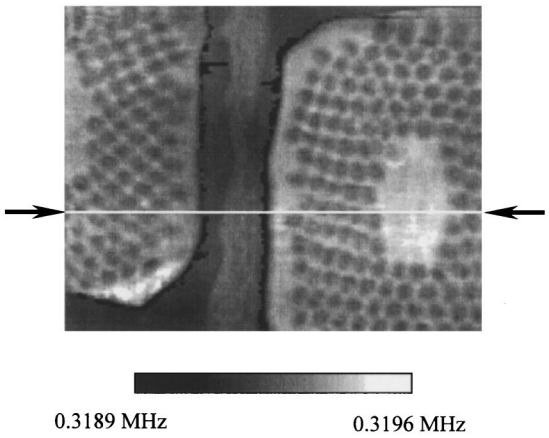

FIG. 7. RUM image of superconductive wire.

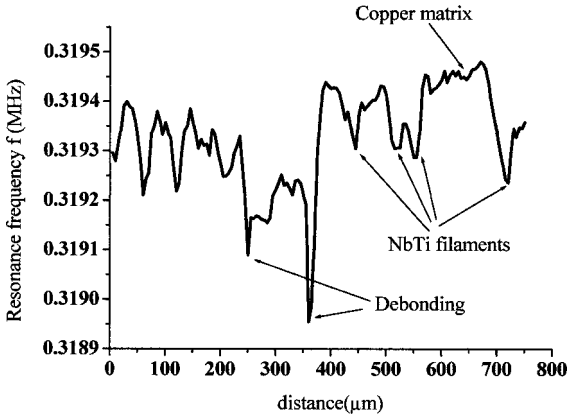

FIG. 8. Line trace of the resonance frequency along the arrowheads shown in Fig. 7.

factor of 2.4–3.6. The static model often used in UAFM studies gives frequency shifts much smaller than measurements. Thus, Fig. 9 demonstrates the capability of the present method for a quantitative relative measurement of local elastic constants. Figures 7 and 8 show the lowest resonance frequency at the copper-resin interfaces, indicating poor bonds or debondings. Such information is unavailable by optical microscopy. Thus, the RUM method has the further potential for nondestructive elevation of a material's deterioration.

V. CONCLUSION

Based on the vibration of a langasite oscillator excited by a one-point-contact acoustic-resonance technique, we developed a resonance-ultrasound-microscopy method for measuring relative elastic constants in a local surface region of solids. The isolated langasite crystal provides an accurate resonance-frequency measurement. Selection of the A_g-1 resonance mode provides high-sensitivity and temperature-stable microscopic methodology. A dynamic-contact model is adopted to predict the resonance frequency of the oscillator, which is suitable for a quantitative evaluation of localized modulus. The method revealed elastic-stiffness distribution of Nb–Ti/Cu/resin superconductive wire. It also

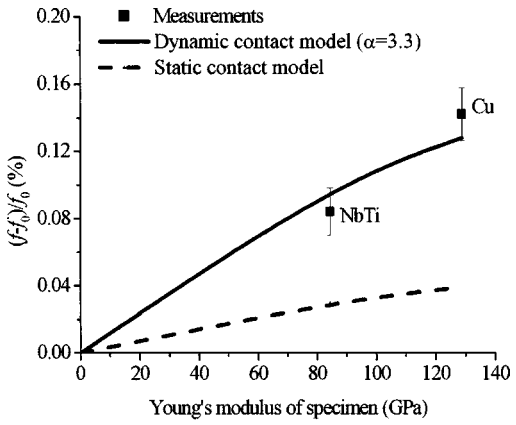

FIG. 9. Comparison of measurements with the dynamic-contact and static-contact models.

revealed the weak bonding at the wire-resin interfaces, showing a potential use for nondestructive evaluation of local damage.

ACKNOWLEDGMENT

J.T. acknowledges the support provided by the Japan Society for the Promotion of Science (JSPS).

[1] X. J. Ning and P. Pirouz, J. Mater. Res. **6**, 2234 (1991).
[2] A. Briggs, *Acoustic Microscopy* (Clarendon, Press Oxford, 1992).
[3] K. Yamanaka, H. Ogiso, and O. Kolosov, Appl. Phys. Lett. **64**, 178 (1994).
[4] U. Rabe, J. Turner, and W. Arnold, Appl. Phys. A: Mater. Sci. Process. **66**, S277 (1998).
[5] H. Ogi, N. Nakamura, K. Sato, M. Hirao, and S. Uda, IEEE Trans. Ultrason. Ferroelectr. Freq. Control **50**, 553 (2003).
[6] A. Bungo, C. Jian, K. Yamaguchi, Y. Sawada, S. Uda, and Y. Pisarevsky, Jpn. J. Appl. Phys., Part 1 **87**, 7491 (2000).
[7] M. Hirao, H. Ogi, and H. Fukuoka, Rev. Sci. Instrum. **64**, 3198 (1993).
[8] H. Ogi, P. Heyliger, H. Ledbetter, and S. Kim, J. Acoust. Soc. Am. **108**, 2829 (2000).
[9] J. Y. Tian, H. Ogi, and H. Hirao, J. Appl. Phys. **95**, 8366 (2004).
[10] I. Ohno, Phys. Chem. Miner. **17**, 371 (1990).
[11] H. Ledbetter, J. Moulder, and M. Austin, Wire J. **31**, 27 (1981).
[12] S. Kim, H. Ledbetter, and H. Ogi, J. Appl. Phys. **88**, 2378 (2000).
[13] C. Reid, J. Routbort, and R. Manynard, J. Appl. Phys. **44**, 1398 (1973).
[14] J. Y. Tian, H. Ogi, T. Tada, and M. Hirao, J. Acoust. Soc. Am. **115**, 630 (2004).